

Segmentation of the vertebrate skull: neural-crest derivation of adult cartilages in the clawed frog, *Xenopus laevis*

Joshua B. Gross^{1,2} and James Hanken

Department of Organismic and Evolutionary Biology and Museum of Comparative Zoology, Harvard University, 26 Oxford St., Cambridge, MA 02138, USA

Synopsis We utilize a novel, transgenic cell-labeling system to assess the embryonic derivation of cartilages in the post-metamorphic skull of anuran amphibians. Many of these cartilages form *de novo* at metamorphosis and have no obvious precursors within the larval skeleton. Most adult cartilages are derived from mandibular- or hyoid-stream neural crest, either individually or in combination; branchial-stream neural crest makes a modest contribution. Each stream also contributes to at least one cartilage in the middle ear or external ear. Four cartilages are composite elements; each is derived from at least two distinct cell populations. Many boundaries between adjacent neural-crest territories are cryptic insofar as they do not coincide with anatomical boundaries. The system of adult cranial segmentation revealed by these fate-mapping results differs in important respects from both the segmentation of the ontogenetically earlier larval skull and the cranial segmentation in amniotes. Most striking is the rostral “inversion” of neural-crest-derived cartilages in *Xenopus*, such that mandibular stream-derived elements are deployed caudal to those derived from the hyoid stream, which predominate anteriorly. This novel pattern of rostral segmentation may be a consequence of the complex, biphasic life history that is characteristic of most species of living amphibians, and especially anurans, in which cranial architecture is significantly reconfigured at metamorphosis. Neural-crest derivation of the vertebrate skull is not invariant; instead, embryonic derivation of individual components of the cranial skeleton may vary widely among species.

Introduction

Arguably there is no more “classical” a topic in anatomy and evolutionary biology than segmentation of the vertebrate head (Hanken and Hall 1985). Early theories and accounts of head segmentation focused on the bony adult skull and its possible correspondence to modified vertebrae (Owen 1866; Gegenbaur 1872; reviewed by de Beer 1937; Jollie 1977). These treatments were subsequently expanded to include other skeletal and non-skeletal tissues in both adults and embryos (Goodrich 1930; Bjerring 1967), and such analyzes continue to the present day (Kuratani 2003, 2005; Kuratani and Ota 2008). Yet, despite intense study of this problem by many of the foremost developmental biologists and anatomists of the last 200 years, a comprehensive understanding of head segmentation in any vertebrate species remains elusive. Even further from our grasp is characterization of the extent to which head segmentation may vary across vertebrate phylogeny or in response to adaptation for cranial function or for organismal life history.

The nature and extent of segmentation of the vertebrate skull has been especially difficult to resolve, particularly in adults, largely because of the paucity of fundamental data regarding the embryonic origin of the two primary cranial-skeletal tissues, cartilage and bone (Gross and Hanken 2008). Whereas a significant literature extending back more than a century has successfully revealed the derivation of much of the cartilaginous viscerocranium (pharyngeal-arch skeleton) from embryonic neural crest (Platt 1893; Landacre 1921; Stone 1926, 1929; Hörstadius 1950; Chibon 1967; Sadaghiani and Thiébaud 1987), comparable mapping of the derivation of adult cartilages and bones from neural crest or from cranial mesoderm has only been achieved much more recently (Johnston et al. 1973; Le Lièvre 1978; Noden 1984; Couly et al. 1993; Köntges and Lumsden 1996; reviewed by Le Douarin and Kalcheim 1999; Morriss-Kay 2001; Jiang et al. 2002; Gross and Hanken 2008). The latter studies, at present limited to the two primary amniote models, mouse and chicken, were enabled by the application

From the symposium “Vertebrate Head Segmentation in a Modern Evo-Devo Context” presented at the annual meeting of the Society for Integrative and Comparative Biology, January 2–6, 2008, at San Antonio, Texas.

¹E-mail: jgross@genetics.med.harvard.edu

²Present address: Harvard Medical School, Department of Genetics, Boston, MA 02115, USA

Integrative and Comparative Biology, volume 48, number 5, pp. 681–696

doi:10.1093/icb/icn077

Advance Access publication August 2, 2008

© The Author 2008. Published by Oxford University Press on behalf of the Society for Integrative and Comparative Biology. All rights reserved. For permissions please email: journals.permissions@oxfordjournals.org.

of novel methods for long-term labeling of embryonic cell populations and reliably tracing their contributions to the adult skeleton (Le Douarin and Barq 1969; Noden 1984; Chai et al. 2000). Ironically, until very recently such methods have not been available for amphibian models, which were the predominant subjects of early fate-mapping studies (see references above). Consequently, to date, there is almost no direct, empirical evidence of the embryonic derivation of adult cartilages and bones in amphibians, many of which form *de novo* at metamorphosis and have no obvious precursors within the larval skeleton (Carl et al. 2000; Gross and Hanken 2004, 2005, 2008; Pugener and Maglia 2007).

Here, we present new data regarding the long-term contributions of cranial neural crest to the persistent cartilages of the post-metamorphic skull of the clawed frog, *Xenopus laevis*. We utilize a standard technique for grafting pre-migratory streams of cranial neural crest in embryos in combination with a novel transgenic line of frogs, which provides a permanent and reliable cell label that is effective for tracing the embryonic derivation of adult structures that may not form until days, weeks or even months after hatching (Borchers et al. 2000; Gross and Hanken 2004; Gross et al. 2006). In combination with additional data regarding the long-term contributions of cranial neural crest to the adult osteocranium (Gross and Hanken manuscript in preparation), these results provide insights into the pattern of segmentation of the adult skull of anurans, which differs in significant respects from the segmentation of the earlier larval skull and from the segmentation of the skull in amniotes.

Methods

Neural-crest grafts

We grafted “labeled” explants of premigratory cranial neural crest from transgenic (*ROSA26:GFP*) donor embryos into unlabeled, stage-matched, wild-type hosts following established procedures (Gross and Hanken 2004, 2005; Gross et al. 2006). A given explant contained neural crest that contributes to a single cranial migratory stream—mandibular, hyoid, or branchial—as determined in previous studies (Olsson and Hanken 1996; Gross and Hanken 2004, 2005). Two sets of grafts roughly three months apart were performed using labeled offspring from the same transgenic F₀ female founder. Both this female and a wild-type (non-transgenic) adult female were primed to mate with simultaneous injections of 500 µl of human chorionic gonadotropin (Sigma Aldrich, St. Louis, MO, USA). To obtain

stage-matched donors and hosts, *in vitro* fertilizations of transgenic and non-transgenic eggs were performed simultaneously using sperm from a single, wild-type male. In the *ROSA26:GFP* transgenic strain, the GFP construct is widely expressed in all cell types examined, at all stages of the life history (Gross et al. 2006). We used only the most brightly fluorescing embryos as donors.

Embryonic grafts were carried out in Modified Barth Saline (high salt) Solution (MBSH; Sive et al. 2000). Each graft was performed unilaterally, on the right side. A small portion of the neural crest was removed from a wild-type host embryo and replaced with a similar-sized graft from the corresponding region from a transgenic donor (Gross et al. 2006). In each case, only neural crest was removed, leaving the overlying ectoderm intact. Before and after surgery, embryos were reared at room temperature in 0.1 × Marc’s Modified Ringer’s solution (MMR; Sive et al. 2000). Accuracy of each graft was assayed the following morning; duration of fluorescence exposure was minimized to avoid potential damage from UV irradiation. After about 1 week, the now-tadpoles (approximately NF stage 42; Nieuwkoop and Faber 1994) were again briefly illuminated to verify which neural-crest migratory stream was labeled with *ROSA26:GFP*-expressing cells.

A separate series of grafting experiments using fluorescent-dextran-labeled donor embryos and explants was performed in parallel to the transgenic grafts to verify the accuracy and specificity of the grafting procedure, which otherwise was identical to that described above. These experimental animals were sacrificed at day 5 (approximately NF stage 41) and assayed to confirm the presence of labeled cells in the cartilaginous larval viscerocranium. Results (data not shown) were identical to those of earlier studies regarding both the overall extent of the neural crest’s contribution to the anuran viscerocranium and the stream-by-stream derivation of individual cartilages (Stone 1929; Sadaghiani and Thiébaud 1987; Olsson and Hanken 1996). This includes absence of labeling in the basibranchial (or “cupola”), an unpaired cartilage in the ventral midline that shows no evidence of neural-crest derivation and instead is presumed to be derived from cranial mesoderm.

Animal husbandry and rearing

Tadpoles were reared in groups according to the type of cranial neural-crest explant and to the labeled migratory stream(s) as determined above. For example, the “mandibular” group was derived from

embryos that received grafts of premigratory mandibular crest and which expressed GFP exclusively in the mandibular stream. Some explants contained neural-crest cells that populated (and labeled) two adjacent migratory streams; the corresponding tadpoles were also maintained separately, e.g., “mandibular + hyoid” group.

Each group was reared in a separate 8-gal tank that received fresh 10% Holtfreter solution filtered through a carbon filter, mechanical filter and biofilter (Marine Biosystems, Beverly, MA, USA). Time to metamorphosis varied among individuals, and there was some attrition within each group between the time of grafting and the completion of metamorphosis. When possible, experimental animals were reared for 10–12 weeks, by which time all individuals had completed metamorphosis (NF Stage 66) and ossification of nearly all skull bones had begun (Trueb and Hanken 1992). The first set of grafts was performed on June 9, 2004 and all surviving individuals were sacrificed on August 17 of that year. The second set of experiments was performed on September 30, 2004 and all surviving individuals were sacrificed on January 3, 2005.

Animal care procedures are approved by the Harvard University/Faculty of Arts and Sciences Standing Committee on the use of Animals in Research and Teaching. An Animal Welfare Assurance statement is on file with the university's Office for Laboratory Welfare (OLAW). Experimental animals were sacrificed by brief immersion in 1% aqueous tricaine methanesulphonate (MS-222; Sigma-Aldrich, St. Louis, MO, USA) and immediately fixed in fresh 3.7% paraformaldehyde/PBS (pH 7.4–7.6) at 4°C. The following morning, they were rinsed completely in fresh PBS (pH 7.4) and stored in PBS at 4°C until processing.

Histological processing and staining

Following fixation and rinsing, each specimen was processed to remove the skin and soft tissues that surround the cranium. The skull was carefully separated from the vertebral column and carefully dissected clear of remaining soft tissues (e.g., muscles, connective tissue) while leaving all skeletal tissues intact. It was then placed in Optimal Cutting Temperature (OCT) cryomedium and frozen in a plastic mold at –80°C. Frontal sections (16–20 µm) were cut on a Leica CM 3050S cryostat, collected onto VWR Superfrost slides, allowed to dry for 1 h at room temperature, and then frozen at –80°C until antibody staining. Successive sections were collected and processed in three sets, or series. Set 1 was

processed for normal indirect immunohistology using a polyclonal, anti-GFP antibody. Set 2 (control) was processed with no secondary antibody. Set 3 was processed for bone and cartilage using a TriChrome staining protocol (Presnell and Schreibman 1997).

All antibody staining used the following protocol: 2 h, room-temperature block in 5% normal goat serum in PBS + 0.1% Triton X-100, then primary antibody incubation overnight (14–18 h) at 4°C (Rabbit anti-GFP; Torrey Pines Biolabs, Temecula, CA, 1:500; and/or Abcam Antibodies, Cambridge, MA, 1:1000), followed by several rinses in PBS + 0.25% Triton X-100 at room temperature for 4–6 h.

Secondary antibody was diluted 1:500 in PBS + 0.1% Triton X-100 and incubated overnight at 4°C (goat anti-rabbit Alexa 488; Probes, Eugene, OR, USA). The following morning, slides were rinsed several times in PBS + 0.25% Triton X-100 at room temperature for 4–6 h. They were then incubated for 10 min in Hoechst 33,342 nuclear counterstain (Probes, Eugene, OR, USA) in PBS + 0.25% Triton X-100 and mounted with a glass coverslip using Fluoromount G (Southern Biotech, Birmingham, AL, USA).

Trichrome-stained slides (Presnell and Schreibman 1997) were mounted using Cytoseal 60.

Microscopy and tissue analysis

Sectioned tissues were analyzed to determine the nature and extent of the cellular contribution of cranial neural crest to adult cranial cartilages. Each section of every skull was examined with fluorescence microscopy (Leica model DMRE equipped with B-filter; Leica, Bannockburn, IL, USA) and the presence or absence of positive GFP labeling was recorded for each cartilage. Several steps were taken to control for false positives: (1) staining was examined in the same cartilage on the contralateral (left) side of the skull, which had not received a labeled graft; (2) staining was compared to the same structure on the adjacent slide processed for immunohistochemistry but without secondary antibody (the only background fluorescence detected as a function of the staining protocol was attributable to the secondary antibody); and (3) the comparable region on the slide-set processed with TriChrome stain was examined to ensure that the positive GFP label was located within cartilage matrix. Confirmed instances of positive labeling within cranial cartilages are listed in Table 1.

There was relatively little variation in the pattern of cartilage labeling among specimens of a given

Table 1 Cranial neural-crest contribution to cartilages in the adult (post-metamorphic) skull of *Xenopus laevis*. Individual cranial cartilages are listed according to the neural-crest stream(s) from which they are derived. Sample size (*n*) denotes the number of specimens in which GFP-labeled cells were observed

Cartilage	Migratory stream(s)	<i>n</i>
Palatoquadrate	Mandibular	6
Tympanic annulus	Mandibular	1
Meckel's cartilage	Mandibular/hyoid	4/1
<i>Planum antorbitale</i>	Mandibular/hyoid	6/4
<i>Septum nasi</i> (caudal to median prenasal process)	Mandibular/hyoid	2/4
<i>Septum nasi</i> (median prenasal process)	Hyoid	3
<i>Tectum nasi</i>	Hyoid	3
<i>Solum nasi</i>	Hyoid	3
Alary cartilage	Hyoid	2
Inferior prenasal cartilage	Hyoid	3
Oblique cartilage	Hyoid	3
<i>Planum terminale</i>	Hyoid	3
<i>Pars externa plectri</i>	Hyoid	2
<i>Pars media plectri</i>	Hyoid	2
<i>Pars interna plectri</i>	Branchial	2
Otic capsule (anterior, within prootic bone)	Branchial	6
Otic capsule (posterior, within exoccipital bone)	Branchial	3

graft type. We interpret this variation to reflect slight but inevitable differences in the size of labeled (donor) explants and in the exact location of grafts in unlabeled (host) embryos. Each of these features may affect the subsequent migration of both labeled and unlabeled neural-crest cells. Variation in labeling pattern, when present, is reported below (Results).

Acquisition of images

Fluorescent images were compiled using the merge function in Openlab (Improvision; Boston, MA, USA). Each time a positive label was detected within the cartilaginous matrix, a black-and-white Nomarski image was captured, along with a pseudo-Green-colored fluorescent image of the same section of cartilage. Each pair of images was then merged in Openlab. Figures below present images of the experimentally grafted side opposite those of the control, ungrafted side.

Anatomical terminology

Anatomical terminology follows that used for *X. laevis* by Trueb and Hanken (1992). This terminology is

consistent with the online anatomical lexicon being developed for Recent amphibians, Amphibian Anatomical Ontology (www.amphibanat.org), which, with few exceptions, embraces standard terminology used previously for other species of anurans (e.g., Jurgens 1971; Reiss 1998).

Results

Contributions from mandibular-stream neural crest to adult cranial cartilages

GFP-expressing chondrocytes derived from labeled grafts of mandibular-stream neural crest were observed in five adult cranial cartilages (Table 1; Fig. 1). The mandibular stream was the exclusive source of labeled cells for two of these cartilages, the palatoquadrate rostrally and tympanic annulus caudally, whereas the remaining three cartilages—*septum nasi*, *planum antorbitale*, and Meckel's—each received additional contributions from the hyoid stream (see below).

All regions of the extensive palatoquadrate cartilage were labeled in one specimen or another, including the posterior maxillary process, pterygoid process, remnants of the larval ventrolateral process, and cartilage cells adjacent to the ossified *pars articularis* of the quadrate bone (Fig. 2).

All grafts of mandibular-stream neural crest labeled Meckel's cartilage, and contributions from these cells were noted along the element's entire length in one specimen or another (Fig. 3B, D, and F). Labeling frequently presented a pattern in which clusters of labeled cells alternated with similarly sized clusters of unlabeled cells along the anteroposterior axis, especially in the intermediate, elongated portion of the element (Fig. 3D). This pattern suggests that the cartilaginous lower jaw of the larva elongates through a process of clonal expansion of crest-derived chondrogenic cells, perhaps triggered by the onset of metamorphosis. As noted below, a small contribution from hyoid-stream-derived cells to the articular region of Meckel's cartilage was seen in one specimen (Fig. 3H).

Contributions to the tympanic annulus in the external ear are described below.

Contributions from hyoid-stream neural crest to adult cranial cartilages

GFP-expressing chondrocytes derived from labeled grafts of hyoid-stream neural crest were observed in nine anterior cartilages (Table 1; Figs. 1, 3–6): Meckel's cartilage (articular region only), *planum antorbitale*, *septum nasi* (especially ventrally, and in the median prenasal process anteriorly), *tectum nasi*,

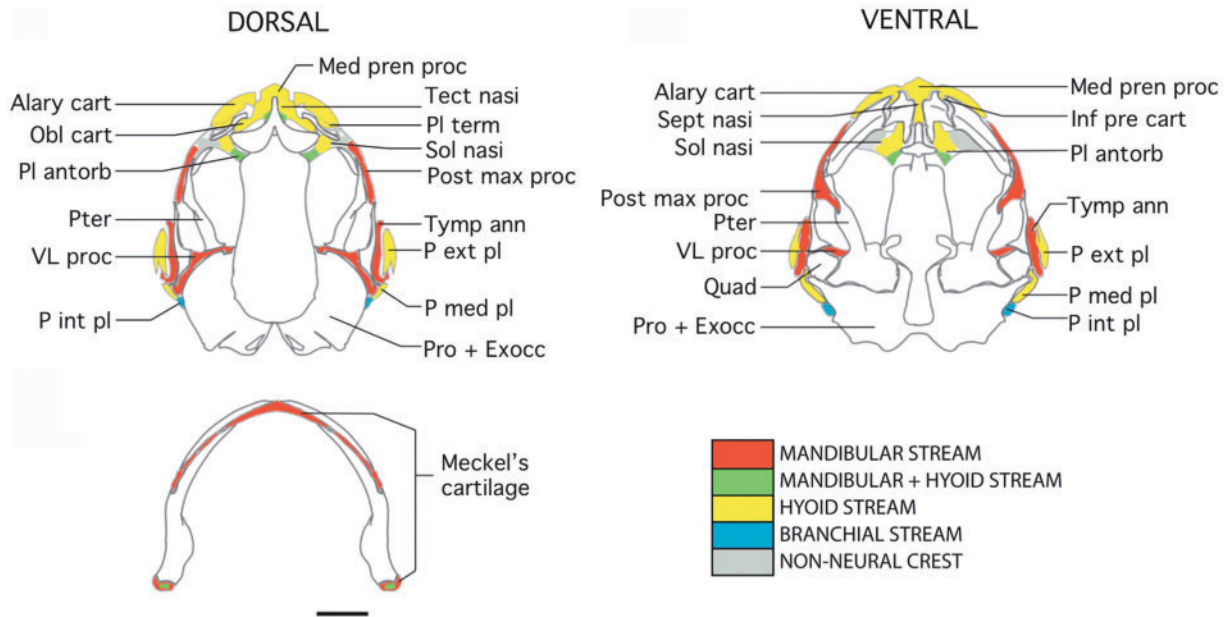


Fig. 1 Schematic fate map depicting stream-level contributions of cranial neural crest to cartilages in the post-metamorphic skull of *X. laevis* (NF Stage 66 + 1 month). The map combines data collected from a series of experiments and numerous specimens (see Methods) as summarized in Table 1. Outline drawing of skull modified from Trueb and Hanken (1992). Cartilages are shaded; bones are unshaded (white). Scale bar, 2 mm. Alary cart, alary cartilage; Exoc, exoccipital bone; Inf pre cart, inferior prenasal cartilage; Med pren proc, median prenasal process (of septum nasi); Obl cart, oblique cartilage; P ext pl, *pars externa plectri*; P int pl, *pars interna plectri*; Post max proc, posterior maxillary process; P med pl, *pars media plectri*; Pl antorb, *planum antorbitale*; Pl term, *planum terminale*; Pro, prootic bone; Pter, pterygoid process; Quad, *pars articularis* of the quadrate bone; Sept nasi, *septum nasi*; Sol nasi, *septum nasi*; Tect nasi, *tectum nasi*; Tymp ann, tympanic annulus; VL proc, ventrolateral process.

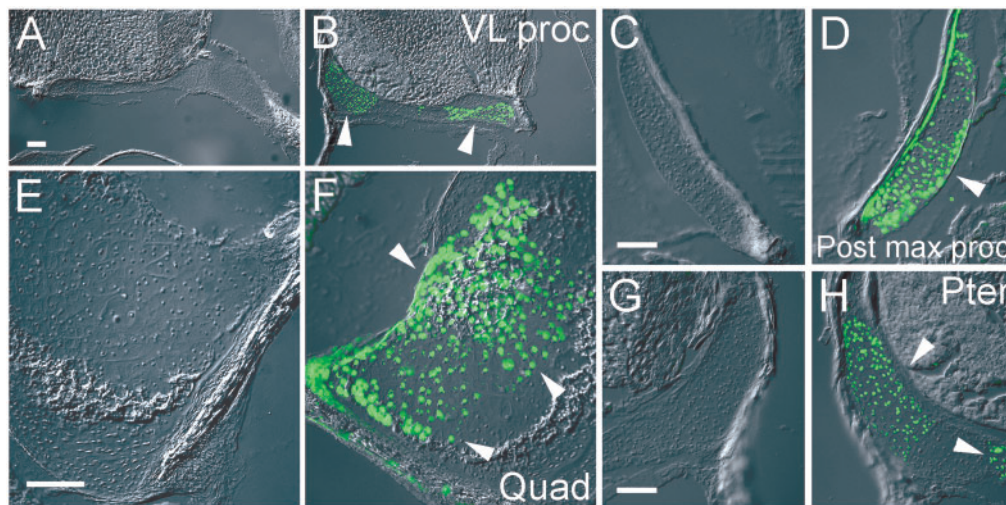


Fig. 2 Mandibular-stream neural crest contributes to the adult palatoquadrate cartilage. GFP-positive cells (green) are present in remnants of the larval ventrolateral process (**B**; VL proc), posterior maxillary process (**D**; Post max proc), pterygoid process (**H**; Pter), and the still-cartilaginous core of the *pars articularis* of the quadrate bone (**F**; Quad). Frontal sections, anterior at top; images are arranged in pairs (**A**, **B**; **C**, **D**; etc.) with the right (grafted) side of a given specimen on the right-hand side, opposite the left (control) side of the same specimen. Fluorescently labeled cartilage cells were only observed on the right side in each specimen. Scale bar, 1 mm.

solum nasi (medial portion only), alary cartilage (medial and lateral aspects), inferior prenasal cartilage, oblique cartilage, and *planum terminale*. Hyoid-stream contributions were also observed in two middle-ear cartilages in the posterior portion of the

skull, the *pars externa plectri* and *pars media plectri* (see below).

For most of the above cartilages hyoid-stream labeling was present throughout each element, but in four cases certain regions of a given cartilage

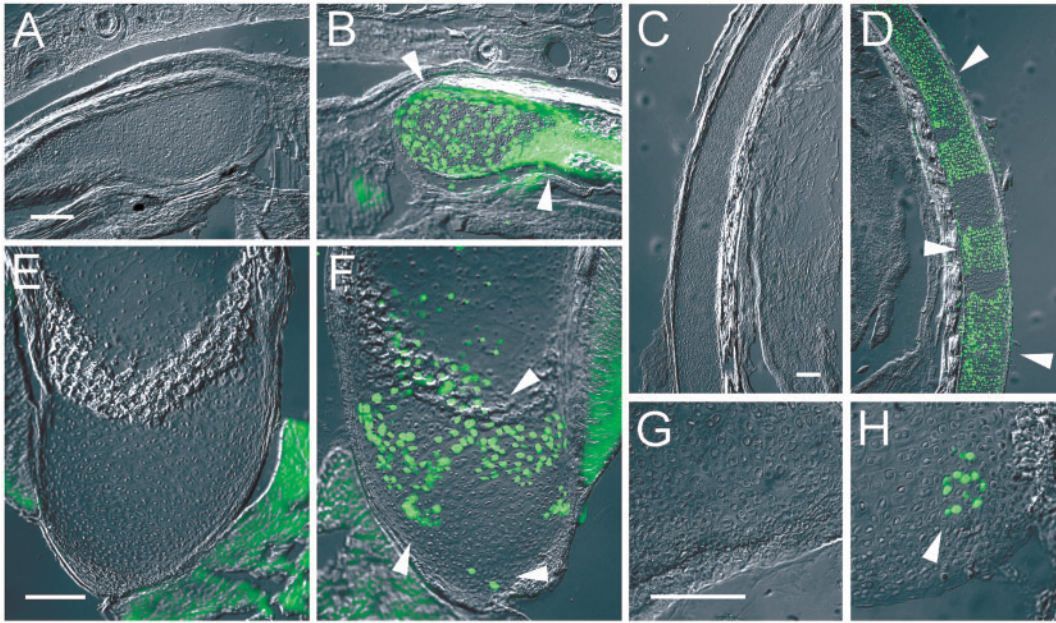


Fig. 3 Neural-crest derivation of the cartilaginous lower jaw of adult *Xenopus*. GFP-positive cells derived from labeled explants of premigratory, mandibular-stream neural crest are found throughout Meckel's cartilage: (A, B) transverse section through anterior ramus; (C, D) frontal section through elongate body, anterior at top; (E, F) frontal section through posterior tip (jaw articulation). (G, H) A few labeled cells were seen in the posterior tip in one of six individuals that received a hyoid-stream graft. Images are paired as in Fig. 2. Fluorescently labeled cartilage cells were only observed on the right side in each specimen. Scale, 1 mm.

consistently lacked GFP-expressing cells. Three of these are the *septum nasi*, *planum antorbitale*, and Meckel's cartilage, all of which receive additional contributions from the mandibular stream (see below). Indeed, a hyoid-stream contribution to Meckel's cartilage was noted in just a single specimen that had a tiny cluster of GFP-expressing cells at the most posterior (articular) portion of the lower jaw. The hyoid-stream contribution to the *solum nasi*, however, was consistently restricted to its medial portion (Fig. 4I). We obtained no evidence of additional cellular contributions to the lateral portion of this cartilage from the hyoid or any other cranial neural-crest migratory stream.

Composite origin of cranial cartilages from both mandibular and hyoid streams

Three cranial cartilages have a composite neural-crest origin, insofar as each receives contributions from both the mandibular and the hyoid streams. Hyoid-stream-derived cells predominate in the *septum nasi*, especially ventrally and in the median prenasal process anteriorly, where mandibular-stream-derived cells were never observed (Fig. 5A). Dorsally, the *septum nasi* similarly receives its largest contribution from the hyoid stream, although a second, smaller contribution from the mandibular stream is evident

in several specimens caudal to the median prenasal process (Fig. 6A and B).

The *planum antorbitale* comprises similar-sized territories derived from mandibular and hyoid neural-crest streams along its entire proximodistal extent (Fig. 6D and F). We did not observe an anterior versus posterior bias in either cell population within this cartilage. Instead, cells from both streams appear to populate the same regions. We have observed, however, differences in the anterior/posterior distribution of cells derived from the mandibular and hyoid streams in the adjacent frontoparietal bone which, when fully formed, extends much further anteriorly and posteriorly (Gross and Hanken 2005).

The tiny contribution of the hyoid stream to the posterior region of Meckel's cartilage observed in a single specimen is described above (Fig. 3H).

Contributions from branchial-stream neural crest to adult cranial cartilages

Contribution of branchial-stream neural crest to adult cranial cartilages is modest in comparison to the much more extensive contributions from mandibular and hyoid streams. GFP-expressing chondrocytes were confined to three paired structures (Table 1): the *pars interna plectri* of the middle ear (see below), and anterior and posterior regions of the

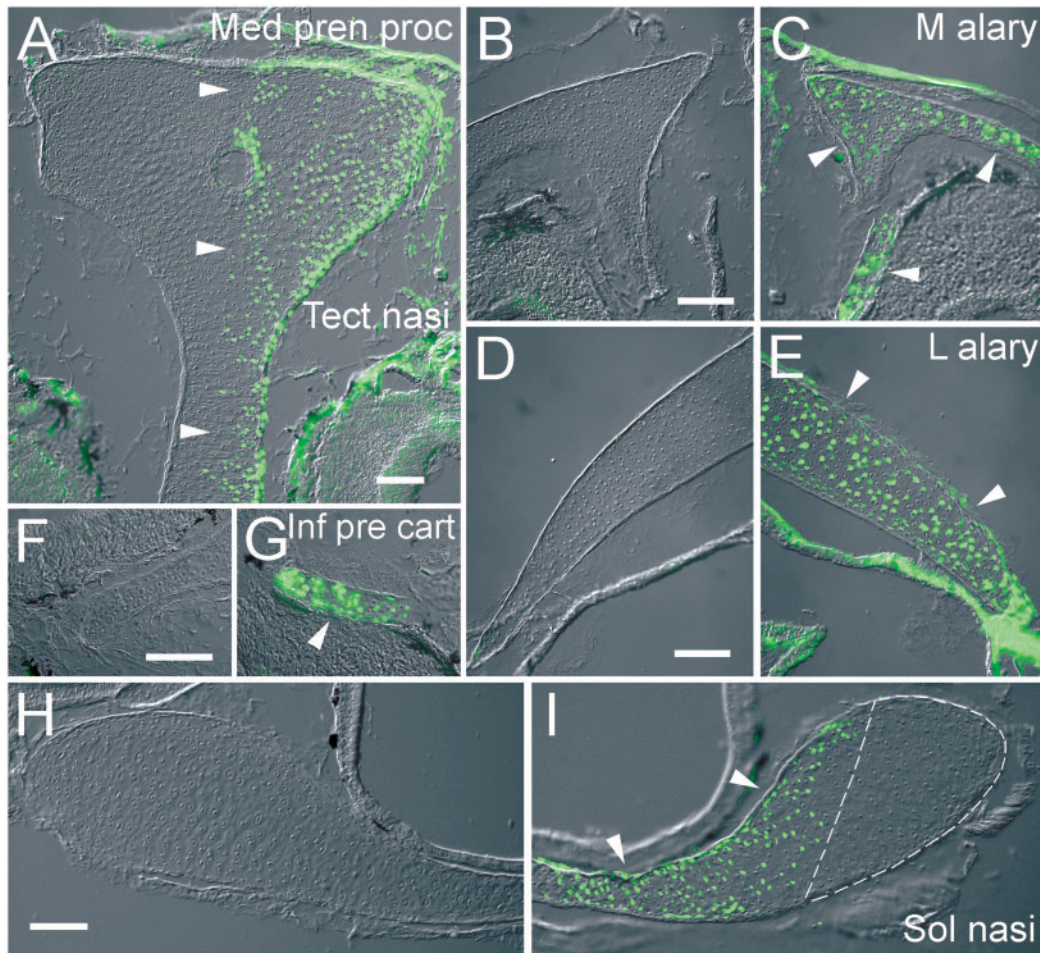


Fig. 4 Contributions of hyoid-stream neural crest to adult cranial cartilages. GFP-labeled cells are present in the median prenasal process (of the *septum nasi*) and, more posteriorly, the *tectum nasi* (A; Med pren proc and Tect nasi, respectively); the medial and lateral alary cartilages (C, E; M alary and L alary, respectively); the inferior prenasal cartilage (G; Inf pre cart); and the *solum nasi* (I; Sol nasi). (A–I) frontal sections, anterior at top; B–I are paired as in Fig. 2. Fluorescently labeled cartilage cells were only observed on the right side in each specimen. However, the lateral region of the *solum nasi* on the grafted side was never populated by labeled neural crest from any cranial stream (I; dashed line). Scale bar, 1 mm.

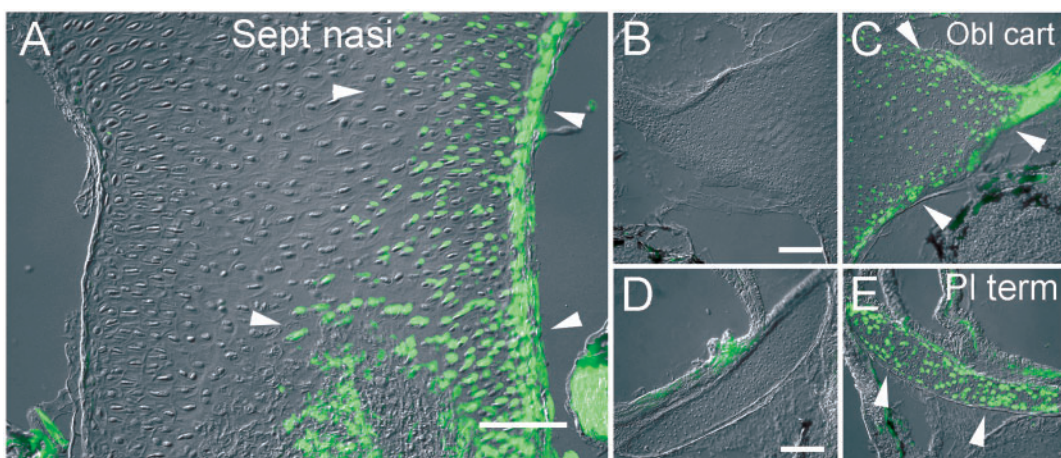


Fig. 5 Contributions of hyoid-stream neural crest to adult cranial cartilages (continued). GFP-labeled cells are present in the ventral portion of the *septum nasi* (A; Sept nasi), in the oblique cartilage (C; Obl cart), and in the *planum terminale* (E; PI term). (A) frontal section; anterior at top. (B–E) transverse sections; images paired as in Fig. 2. Fluorescently labeled cartilage cells were only observed on the right side in each specimen. Scale bar, 1 mm.

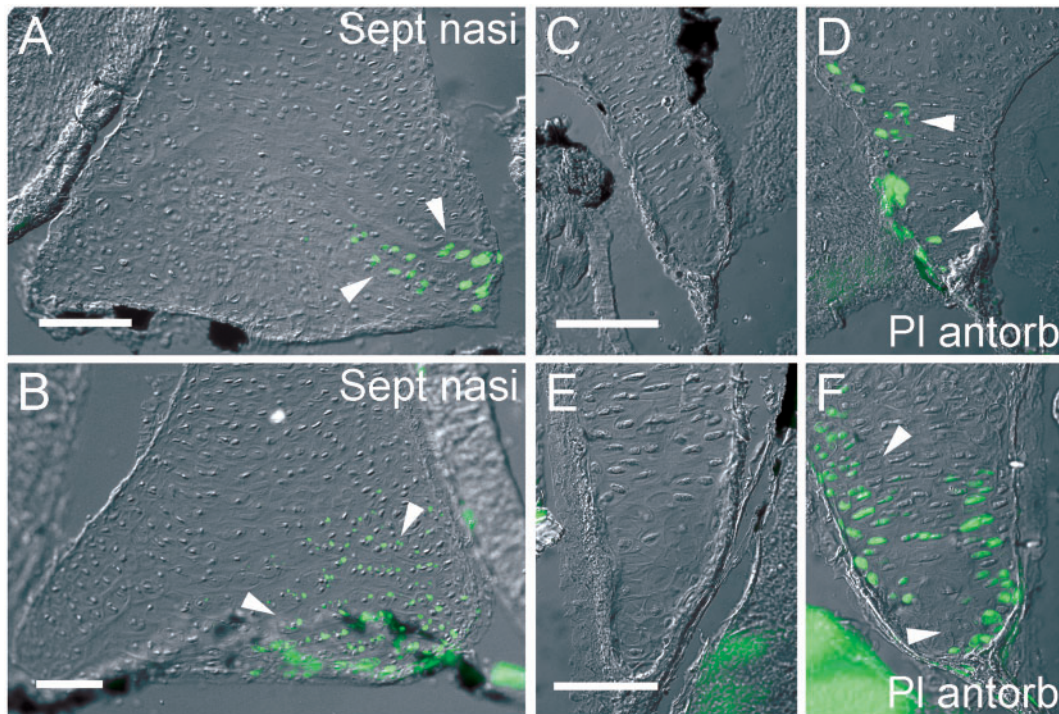


Fig. 6 Three adult cartilages each receive contributions from two cranial neural-crest streams. GFP-positive cells are localized to the same posterolateral and dorsal region of the *septum nasi*, regardless of whether the cells are derived from grafts of mandibular (A; *Sept nasi*) or hyoid (B) streams. As shown here, the hyoid stream typically contributes more cells and populates a larger area. Similarly, the *planum antorbitale* receives contributions from both mandibular and hyoid neural-crest streams (D and F, respectively; PI antorb). (A) and (B) are frontal sections, anterior at the top; each section depicts right and left sides. (C–F) are frontal sections, paired as in Fig. 2. Fluorescently labeled cartilage cells were only observed on the right side in each specimen. Scale bar, 1 mm. Mandibular-stream and hyoid-stream contributions to Meckel's cartilage are depicted in Fig. 3.

otic capsule (Fig. 7). Labeled cells within the otic capsules were patchily distributed and associated with the incompletely ossified prootic and exoccipital bones.

Neural-crest contributions to cartilages of the external ear and middle ear

A complex of five small cartilages contributes to the otic apparatus (external and middle ear) in many adult frogs, including *X. laevis*: tympanic annulus, *pars externa plectri* (also known as the extrastapes), *pars media plectri* (stapes proper), *pars interna plectri* (stapedial footplate) and operculum (Trueb and Hanken 1992; Mason and Narins 2002). All five cartilages are absent in larvae and begin to form at metamorphosis; four—all but the operculum—were present in our oldest experimental specimens, which were sacrificed ~1 month after completion of metamorphosis. Most of these cartilages ossify in the full-grown adult, although ossification had not yet begun in our specimens.

Each of the four cartilages present in our specimens receives contributions from a single migratory stream of cranial neural crest. In each instance,

graft-derived cells contribute to only a portion of each cartilage, and labeled and unlabeled portions were consistent among specimens. GFP-expressing cells from the mandibular stream populated the tympanic annulus, a thin, ring-like cartilage that surrounds and supports the tympanum, or eardrum (Fig. 8B). Labeled cells from the hyoid stream populated the *pars externa plectri* and *pars media plectri* (Fig. 8D and F). The former element articulates with the inside of the tympanic membrane distally and with the *pars media plectri* proximally. The *pars interna plectri*, the innermost member of this complex, which conveys vibrations to the oval window of the inner ear, contained cells derived from the branchial stream (Fig. 8H). We obtained no data regarding the derivation of the operculum.

Discussion

Neural-crest derivation of adult cranial cartilages in anuran amphibians

Metamorphic frogs, including the well-studied model, *X. laevis*, have a biphasic life history in which development from single-celled zygote to

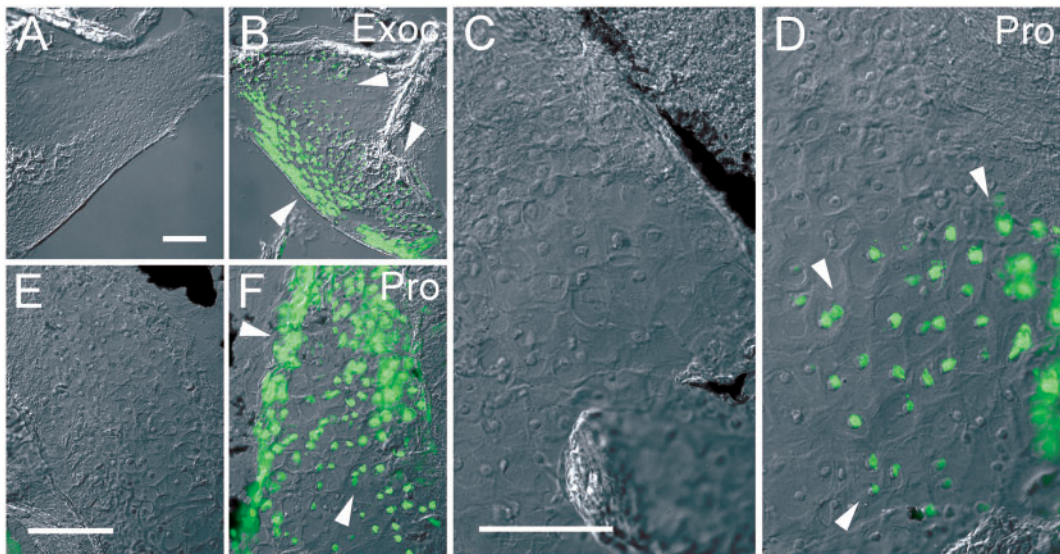


Fig. 7 Contributions of branchial-stream neural crest to the otic capsule. GFP-labeled cartilage cells are present deep in the anterior portion of the exoccipital bone (**B**, arrows upper right; Exoc) and within patches of cartilage remaining in the ossifying prootic bone, (**D**, **F**; Pro). Frontal sections, anterior at the top; images are paired as in Fig. 2. Bone cells also are labeled in (**B**) and (**F**) (left arrow in each). Fluorescently labeled cells were only observed on the right side in each specimen. Scale bar, 1 mm.

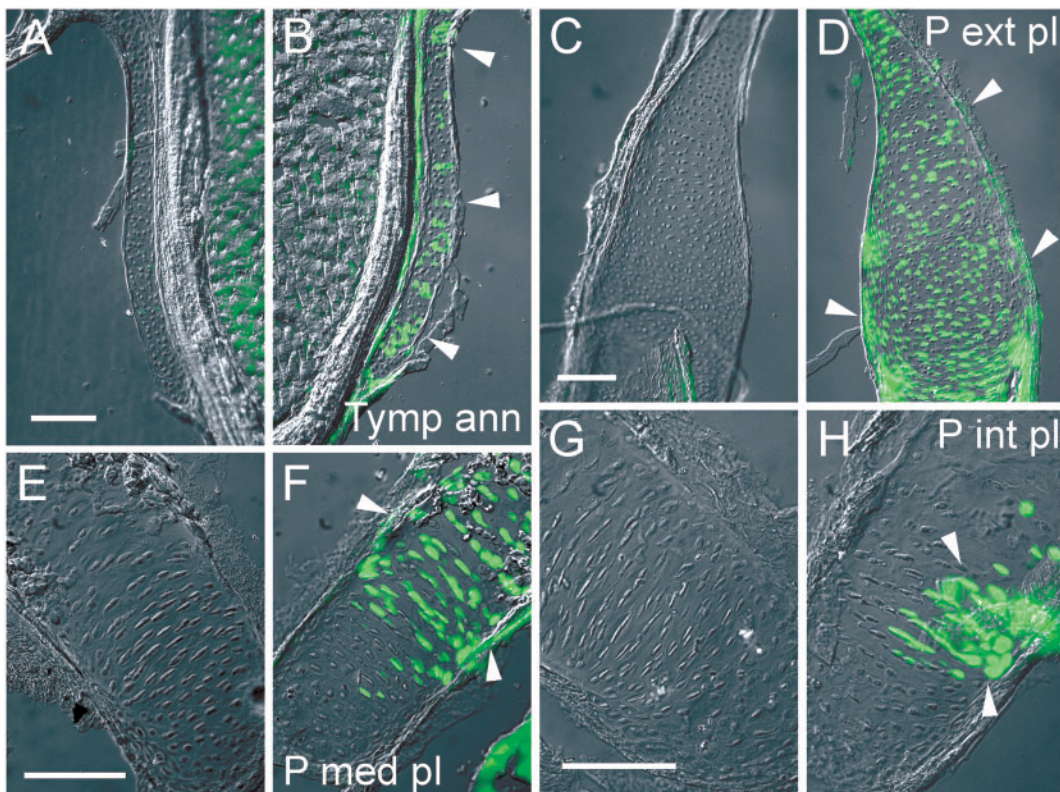


Fig. 8 Complex derivation of otic (external- and middle-ear) cartilages. GFP-labeled cells derived from the mandibular neural-crest stream are patchily distributed in the cartilaginous tympanic annulus (**B**; Tymp ann), whereas hyoid-stream-derived cells contribute to the *pars externa plectri* and *pars media plectri* (**D**, **F**; P ext pl and P med pl, respectively). Only neural-crest cells derived from the branchial stream contribute to the *pars interna plectri* (**H**; P int pl). Frontal sections; images paired as in Fig. 2. Fluorescently labeled cartilage cells were only observed on the right side in each specimen. Scale bar, 1 mm.

sexually mature adult includes a protracted, free-living larval stage (Etkin and Gilbert 1968). Numerous biochemical and morphological changes occur rapidly during metamorphosis, including regression of much of the larval intestine (Nakajima et al. 2005), degeneration of the internal gills and the tail (Tata 1994), and extensive remodeling of the jaw musculature (Haas 2001). Among the most dramatic changes, however, is metamorphosis of the exclusively cartilaginous larval cranium into the compact, bony skull of the adult (Trueb and Hanken 1992). Most larval cartilages are not retained in the adult; many are resorbed, whereas others are replaced by bone, which in metamorphic frogs is an exclusively postembryonic tissue (Hanken and Hall 1984). Simultaneously, several adult-specific cartilages form *de novo*. Most of the cartilaginous nasal capsule of the adult, for example, forms at metamorphosis dorsal to the larval skeleton of the ethmoid region; only a single adult component—the *solum nasi*—is partially retained from the larval skeleton (Pugener and Maglia 2007). In the absence of a reliable cell marker suitable for identifying long-term derivatives of cranial neural crest and other potential embryonic precursors, it has been impossible until very recently to trace the embryonic origin of adult-specific cartilages and bones in the anuran skull (Gross and Hanken 2004, 2008).

We earlier reported a novel transgenic line of *X. laevis* with widespread expression of GFP under the murine *ROSA26* promoter and identified its suitability as a method for long-term labeling of cells in chimeric grafting studies (Gross et al. 2006). We have utilized this method here to assess the pattern of embryonic cranial neural-crest contributions to adult cranial cartilages within the skull proper (Fig. 1). We have not examined the derivation of the adult hyobranchial skeleton, which will be the subject of a future study. Most cranial cartilages in adult *Xenopus* are derived from mandibular-stream or hyoid-stream neural crest, either individually or in combination; branchial-stream neural crest makes a modest contribution to the adult skull. Hyoid-stream derivatives are especially prominent anteriorly, with additional derivatives posteriorly in the middle ear and in the articular region of the lower jaw. Mandibular-stream derivatives within the skull proper are deployed in an intermediate position, essentially between anterior and posterior derivatives of the hyoid stream, although Meckel's cartilage in the lower jaw is derived nearly entirely from mandibular-stream neural crest. Derivatives of the branchial stream are restricted to two sites in the

posterior skull: the middle ear, and cartilaginous remnants of the larval otic capsule.

Four individual cartilages are composite elements insofar as they are derived from at least two distinct populations of cells. Three of these cartilages (*solum nasi*, *planum antorbitale*, Meckel's) appear to be derived entirely from neural crest but each receives contributions from two different migratory streams, mandibular and hyoid. For the fourth cartilage (*solum nasi*), there is evidence of neural-crest derivation to only its medial portion; labeled cells never populated its lateral portion, whose embryonic origin remains unresolved. Additional studies that evaluate directly the contributions of cranial mesodermal and endodermal cells are needed to determine the complete embryonic origin of this element and to document any additional contributions of these cells to the skulls of adult anurans.

Several features of the above pattern in *Xenopus* are unexpected, based on reports of derivation of cranial tissues from the neural crest in other vertebrates (Gross and Hanken 2008). In particular, they differ significantly from data reported for the domestic chicken, the only other vertebrate species that has been examined in comparable detail (Le Lièvre 1978; Noden 1978, 1984; Couly et al. 1993). For example, the complex of nasal and other rostral cartilages, which constitute the anteriormost region of the skull in adult frogs, is derived exclusively from cells of the hyoid migratory crest stream and not from the mandibular stream, which is the primary embryonic source of the rostral skull in chickens. The posterior boundary of neural-crest-derived cartilages within the adult skull also extends much further posteriorly in *Xenopus* to include cartilaginous remnants of the larval otic capsule within both the prootic and exoccipital bones. The exoccipital bone is reported to be a mesodermal derivative in chickens (reviewed by Gross and Hanken 2008).

Embryonic derivation of the middle ear and external ear

There is a large literature that extends back well over a hundred years regarding the developmental origin of the cartilages of the middle- and external-ear in living amphibians (reviewed by Barry 1956; Sedra and Michael 1959; van der Westhuizen 1961; Swanepoel 1970). The origin of the stapes (columella), in particular, and the pharyngeal arch with which it is most closely associated, has been "an old and vexing problem," and as recently as 1963, Toerien (1963, p. 468–469) stated: "The ontogenetic

evidence is uncertain and . . . interpretations based on the study of developmental series of numerous amphibians are widely divergent.” Today, the prevailing view regards the stapes (including the *pars interna plectri*, *pars media plectri*, and *pars externa plectri*) of the middle ear as a second (hyoid)-arch component and the tympanic annulus of the external ear as a first (mandibular)-arch component, although numerous alternative hypotheses have been offered at one time or another (Swanepoel 1970).

Most previous studies attempted to trace the origin of middle- and external-ear cartilages from skeletal elements of the mandibular arch or hyoid arch that are present in the aquatic larvae of metamorphosing species. Their principal goal was to establish homologies both among otic elements found in the three orders of Recent amphibians—frogs, salamanders, and caecilians—and from these elements to comparable structures in fishes and archaic amphibians as a means of understanding the evolution of tetrapod vertebrates (Hetherington 1987). Nearly all of these studies, however, were conducted before the general acceptance or even widespread recognition of the predominant contribution of the embryonic neural crest to the vertebrate skull (Hall and Hanken 1985) and before the advent of reliable experimental methods that enable the embryonic derivation of otic cartilages and other adult-specific features to be traced reliably (Gross and Hanken 2004). Consequently, few purport to directly trace any of the otic elements to their embryonic precursors, as we have done in this study (e.g., Toerien 1963).

Our results substantiate in large part, but not completely, the prevailing view regarding the pharyngeal-arch “identity” of the four otic cartilages we consider. The tympanic annulus is derived from mandibular-stream neural crest, as would be expected for a mandibular-arch component. Likewise, the *pars externa plectri* and *pars media plectri*, two hyoid-arch components, are derived from hyoid-stream neural crest. Branchial-stream derivation of the *pars interna plectri*, however, is not expected for a hyoid-arch component. Instead, it reveals the composite embryonic derivation of the stapes, which receives contributions from two adjacent neural-crest streams and not just from the stream that is principally associated with structures of the hyoid arch. Interestingly, the developmental origin of the anuran stapes from the first branchial arch, which is populated by neural crest from the branchial stream, was suggested more than 75 years ago by Violette (1930) based on the location of cartilage differentiation vis-à-vis cranial nerve ganglia and other

soft tissues. This claim was soon discounted by de Beer, who remarked: “it cannot be accepted” (1937, p. 203). In most anurans, all three parts of the stapes form from a single cartilage condensation, but in a few species, including *X. laevis*, the *pars externa plectri* forms a second condensation that is distinct from the one that gives rise to the *pars interna plectri* and *pars media plectri* (Barry 1956; Hetherington 1987). Comparable fate-mapping studies of other species are needed to determine if the composite embryonic origin of the stapes that we report here is related in any way to its formation from distinct chondrogenic foci or to the differential sensitivity of parts of the stapes to experimental perturbation (Luther 1925, discussed in deBeer 1937; Barry 1956). Similarly, it will be very interesting to extend our approach to the origin of the operculum, an additional and prominent middle-ear cartilage, which forms differently in different anuran species (Sedra and Michael 1957, 1959; Hetherington 1987).

Our results generally agree with those from studies of development of the otic region in the domestic chicken (Noden 1982, 1983, 1987, 1988; Couly et al. 1993; Köntges and Lumsden 1996). These comparisons are complicated, however, because the avian studies are not in complete agreement regarding the extent of neural-crest contribution to all individual elements (Gross and Hanken 2008). Studies in chickens also document a complementary contribution of cranial and paraxial mesoderm to middle-ear cartilages, which is not evaluated in the present study.

Segmentation of the anuran skull

There is no single system of segmentation in the skull of metamorphosing anurans. Instead, there are as many as three overlapping or adjacent systems present at any one time, which may involve cartilage and/or bone. Moreover, this complex structural pattern differs dramatically between free-living larvae and adults, and the adult pattern differs in important respects from that reported for other vertebrates.

There are at least two, and likely three, systems of segmentation in the larval skull (Sadaghiani and Thiébaud 1987; Olsson and Hanken 1996). The first corresponds to the fundamental anatomical segmentation of viscerocranial cartilages, i.e., cartilages that form in association with the pharyngeal arches (Fig. 9, right). Beginning rostrally, these cartilages are allied with the first (mandibular) pharyngeal arch, the second (hyoid) arch, and arches three through six; the latter cartilages together constitute the branchial basket, which supports the internal

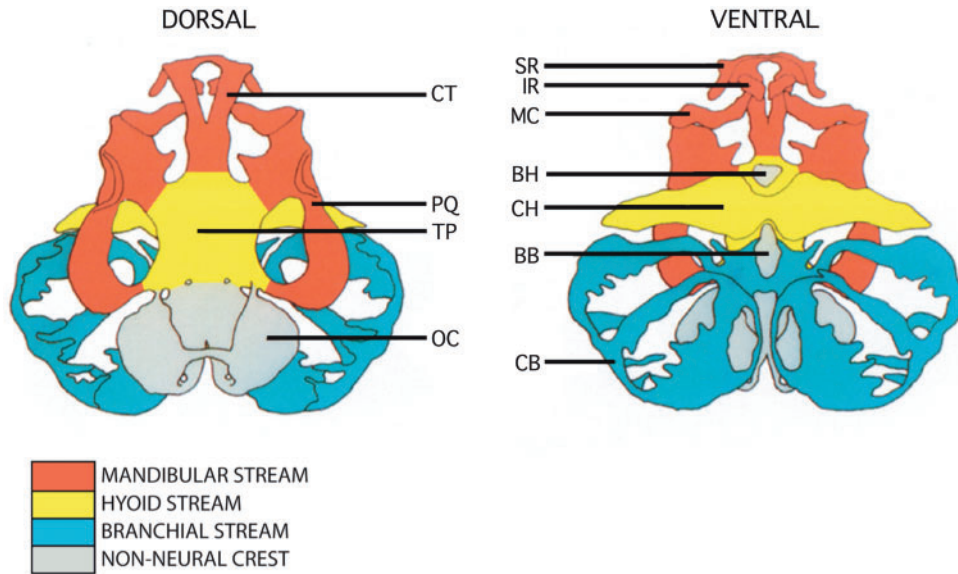


Fig. 9 Neural-crest-associated segmentation of the skull and hyobranchial skeleton in larval frogs. The exclusively cartilaginous skull of the Oriental fire-bellied toad, *Bombina orientalis*, Gosner (1960) stage 36, is depicted in dorsal (left) and ventral views. Cartilages are colored according to the three cranial neural-crest migratory streams from which they are derived; non-crest-derived cartilages are shaded gray. The anterior is located at the top. BB, basibranchial; BH, basihyal; CB, ceratobranchials I–IV; CH, ceratohyal; CT, *cornu trabecula*; IR, infrarostral; MC, Meckel's cartilage; OC, otic capsule; PQ, palatoquadrate; SR, suprarostrals; TP, trabecular plate. Reproduced with permission from Olsson and Hanken (1996).

gills. For the most part, these segments are deployed sequentially from anterior to posterior with little overlap among adjacent segments. The principal exception to this arrangement is the large palatoquadrate cartilage, a first-arch component that extends longitudinally from its anterior articulation with the lower jaw (Meckel's cartilage) to its posterior attachment to the otic capsule.

The second system of cranial segmentation in larval anurans reflects the pattern of neural-crest derivation of the above cartilages and of most cartilages associated with the adjacent neurocranium. Cranial neural crest emerges from the neural tube via three, paired migratory streams, which contribute to most cranial cartilages and nearly all those associated with the pharyngeal arches (Sadaghiani and Thiébaud 1987; Moury and Hanken 1995; Olsson et al. 2002). Indeed, the only arch-associated cartilages that lack a neural-crest derivation are the basihyal and basibranchial, two small elements in the ventral midline (Fig. 9; Stone 1929; Olsson and Hanken 1996). The mandibular stream populates the first arch and contributes to cartilages associated with it and to the rostral neurocranium (Fig. 9, red). Similarly, the hyoid stream populates the second arch and contributes to cartilages associated with it and the adjacent neurocranium (Fig. 9, yellow). Finally, the branchial migratory stream populates

pharyngeal arches 3–6 and contributes to all cartilages of the branchial basket (Fig. 9, blue).

The third system of segmentation comprises occipital and otic cartilages at the caudal end of the skull for which there is no evidence of neural-crest derivation and which presumably are derived from segmented paraxial mesoderm (somites; Fig. 9, gray). The number and identity of such “occipital somites” (O’Rahilly and Muller 1984) that contribute to the posterior skull in different vertebrates, including several species of anurans, is discussed extensively in the classical literature (reviewed by de Beer 1937; see also Smit 1953), and there are a few recent studies that map embryonic origin to specific cell populations using experimental labeling methods. One such fate-mapping study in the larval axolotl, *Ambystoma mexicanum*, documented contributions from occipital somites two and three to cartilage in the cranial and caudal regions of the occipital arch, respectively, as well as to the adjacent atlas vertebra (somite three only; Piekarski and Olsson 2007). Earlier, Toerien (1963) documented a contribution of “axial skeleton” to the medial wall of the otic capsule in a closely related species of salamander, *Ambystoma maculatum*. There are no comparable experimental studies for frogs, but the lack of neural-crest contribution to the otic capsules and adjacent neurocranial cartilages suggests that a similar

derivation of the posterior skull from occipital somites exists in anurans as well. Smit (1953) reviews the histological evidence for segmentation of the posterior (“metotic”) region of the skull in amphibians and reports original data for *X. laevis*. The possible mesodermal derivation of basihyal and basi-branchial cartilages, the sole elements of the larval hyobranchial skeleton that show no evidence of a neural-crest origin, also remains to be assessed experimentally.

The first two segmental systems discussed above overlap extensively. Indeed, both systems define the same mandibular and hyoid segments in the anterior viscerocranium. Intersegmental boundaries of the two systems, however, are not always concordant. Posteriorly, the single “segment” defined by the branchial-neural-crest migratory stream includes cartilages associated with all four posterior pharyngeal arches. A second prominent difference between these two systems concerns the cartilaginous neurocranium. Because the neurocranium lacks any overt physical segmentation, such as that characteristic of the viscerocranium, it is not included within the first, anatomically based system. However, because much of the neurocranium is derived from the neural crest and maintains explicit, albeit cryptic boundaries between territories derived from adjacent migratory streams, it is included in the second, developmentally based system. The paucity of empirical fate-mapping data regarding the contribution of somites to the posterior skull makes it impossible to define the extent of overlap between this presumed (third) system of segmentation and the other two. However, given the small number of cranial bones and cartilages of “mixed” origin (viz., neural crest and mesoderm) documented to date in other vertebrate models (Le Lièvre 1978; Noden 1978, Couly et al. 1993; Matsuoka et al. 2005), we expect that the amount of overlap is small, and that somite-derived components are confined largely, if not exclusively, to the caudal region of the skulls of larval anurans.

The above, relatively simple arrangement of segmental systems in the larva is modified considerably in the skulls of adults. Most obvious is the distortion of the simple rostrocaudal order of the two most cranial segments, at least in the skull proper. Instead of mandibular-stream-derived cartilages predominating rostrally, followed by hyoid-stream-derived cartilages, their relative positions are reversed to a considerable extent. Thus, the most rostral cartilages in the adult neurocranium are derived from the hyoid neural-crest stream and not from the mandibular stream, as would be expected

from the larval configuration (Fig. 1A and B). These are then followed posteriorly by mandibular-stream-derived cartilages, and then by additional hyoid-stream derivatives in the middle ear. Branchial-stream-derived cartilages, which predominate in the larval skull, are virtually absent except for a single element, the *pars interna plectri* in the middle ear. As expected from the distribution of neural-crest-derived segments in the larva, this element lies caudal to cartilages derived from the mandibular and hyoid streams in the skull proper. In the lower jaw, the remnant Meckel’s cartilage is derived exclusively from mandibular-stream neural crest except at its posterior tip, which receives a modest additional contribution from the hyoid stream. While the lower jaw is regarded traditionally as a first-arch element derived solely from the mandibular stream of neural crest, a similar contribution of hyoid-stream neural crest to the articular region (retroarticular process) has been reported in the domestic chicken, in which neural crest also is the source of connective tissues of jaw-opening muscles that attach there (Le Lièvre 1974; Köntges and Lumsden 1996). Thus, composite embryonic derivation of the lower jaw and associated musculature from two adjacent neural-crest streams may be a more widespread feature of vertebrate craniofacial development than previously appreciated (see also Matsuoka et al. 2005).

Life history and cranial evolution

The pattern of segmentation of cranial cartilages in adult anurans, described above, differs in important respects from that reported for other vertebrates. Most striking is the rostral “inversion” of neural-crest-derived cartilages in *Xenopus*, such that mandibular-stream-derived elements are deployed caudal to those derived from the hyoid stream. This arrangement is both unexpected and unprecedented. It reveals a degree of variation in neural-crest derivation of cranial skeletal tissues among species that has been unrecognized previously and therefore challenges the widely held assumption regarding the evolutionary conservatism of patterns of embryonic origin of tissues across vertebrate taxa (Helms et al. 2005). Comparable studies of additional species are needed to establish if our results are unique to *Xenopus*, or if they are typical of frogs or even of amphibians in general. We suggest, however, that the novel pattern of rostral segmentation may be a consequence of the complex, biphasic life history that is characteristic of most species of living amphibians, and especially of anurans, in which

cranial architecture is significantly reconfigured at metamorphosis.

The extent of metamorphic remodeling is especially profound in anurans, in which much of the rostral region of the larval head is first resorbed and then “repopulated” with adult-specific tissues. This includes, for example, the larval upper jaw and its neurocranial support (paired suprarostal cartilages and *cornua trabeculae*; Fig. 9, SR and CT, respectively). These elements are entirely resorbed at metamorphosis and succeeded by a different complex of cartilages and bones, which form *de novo* at that time. These latter elements constitute the adult upper jaw and associated rostral skull. We suggest that in the evolution of this concentrated and extensive burst of postembryonic morphogenesis, the source population of “quiescent” mesenchymal cells that forms the rostral-most elements of the skull switched from mandibular-stream to hyoid-stream neural crest, perhaps as a consequence of the dramatic positional changes inherent to cranial metamorphosis.

Additional studies are required to test this hypothesis. Especially desirable are fine-scale mapping studies that track the migration and differentiation of crest-derived cells throughout metamorphosis to determine when and how skeletogenic cells achieve their final, adult configuration.

Funding

Research presented here was supported by the U.S. National Science Foundation (EF-0334846; AmphibiaTree), The William F. Milton Fund of Harvard University, and a Goelet Summer Research Award from the Museum of Comparative Zoology.

Acknowledgments

We thank Tom Schilling and Shigeru Kuratani for inviting our participation in the Society for Integrative and Comparative Biology symposium on head segmentation in vertebrates. We also thank Nick Marsh-Armstrong and Ericka Oglesby for providing research space and invaluable assistance with grafting experiments.

References

- Barry TH. 1956. The ontogenesis of the sound-conducting apparatus of *Bufo angusticeps* Smith. *Gegenbaurs Morphol Jahrb* 97:477–544.
- Bjerring HC. 1967. Does a homology exist between the basicranial muscle and the polar cartilage? *Colloques Int du Centre Nat de la Recherche Sci* 163:223–67.
- Borchers A, Epperlein HH, Wedlich D. 2000. An assay system to study migratory behavior of cranial neural crest cells in *Xenopus*. *Dev Genes Evol* 210:217–22.
- Carl TF, Vourgourakis Y, Klymkowsky M, Hanken J. 2000. Green fluorescent protein used to assess cranial neural crest derivatives in the frog, *Xenopus laevis*. In: Jacobson C-O, editor. *Regulatory processes in development*. London: Portland Press. p. 167–72.
- Chai Y, Jiang X, Ito Y, Bringas P Jr, Han J, Rowitch DH, Soriano P, McMahon AP, Sucov HM. 2000. Fate of the mammalian cranial neural crest during tooth and mandibular morphogenesis. *Development* 127:1671–9.
- Chibon P. 1967. Nuclear labeling by tritiated thymidine of neural crest derivatives in the amphibian *Pleurodeles waltlii*. *J Embryol Exp Morph* 18:343–58.
- Couly GF, Coltey PM, Le Douarin NM. 1993. The triple origin of skull in higher vertebrates: a study in quail-chick chimeras. *Development* 117:409–29.
- de Beer GR. 1937. *The development of the vertebrate skull*. Oxford: Clarendon Press. p. 552.
- Etkin WE, Gilbert LI. 1968. *Metamorphosis; a problem in developmental biology*. New York: Appleton-Century-Crofts. p. 459.
- Gegenbauer C. 1872. *Untersuchungen zur vergleichenden Anatomie der Wirbelthiere. Drittes Heft. Das Kopfskelet der Selachier, ein Beitrag zur Erkenntniss der Genese des Kopfskeletes der Wirbelthiere*. Leipzig: Wilhelm Engelmann. p. 316.
- Goodrich ES. 1930. *Studies on the structure and development of vertebrates*. London: Macmillan. p. 837.
- Gosner KL. 1960. A simplified table for staging anuran embryos and larvae with notes on identification. *Herpetologica* 16:183–90.
- Gross JB, Hanken J. 2004. Use of fluorescent dextran conjugates as a long-term marker of osteogenic neural crest in frogs. *Dev Dyn* 230:100–6.
- Gross JB, Hanken J. 2005. Cranial neural crest contributes to the bony skull vault in adult *Xenopus laevis*: insights from cell labeling studies. *J Exp Zool B Mol Dev Evol* 304:169–76.
- Gross JB, Hanken J. 2008. A review of fate-mapping studies of the osteogenic cranial neural crest in vertebrates. *Dev Biol* 317:389–400.
- Gross JB, Hanken J, Oglesby E, Marsh-Armstrong N. 2006. Use of a *ROSA26:GFP* transgenic line for long-term *Xenopus* fate-mapping studies. *J Anat* 209:401–13.
- Haas A. 2001. Mandibular arch musculature of anuran tadpoles, with comments on homologies of amphibian jaw muscles. *J Morphol* 247:1–33.
- Hall BK, Hanken J. 1985. *Foreword to G.R. de Beer's, The development of the vertebrate skull*. Chicago: University of Chicago Press. p. vii–xxviii.
- Hanken J, Hall BK. 1984. Variation and timing of the cranial ossification sequence of the Oriental fire-bellied toad, *Bombina orientalis* (Amphibia, Discoglossidae). *J Morphol* 182:245–55.

- Helms JA, Cordero D, Tapadia MD. 2005. New insights into craniofacial morphogenesis. *Development* 132:851–61.
- Hetherington TE. 1987. Timing of development of the middle ear of Anura (Amphibia). *Zoomorphology* 106:289–300.
- Hörstadius S. 1950. The neural crest: its properties and derivatives in the light of experimental research. London: Oxford University Press. p. 111.
- Jiang X, Iseki S, Maxson RE, Sucov HM, Morriss-Kay GM. 2002. Tissue origins and interactions in the mammalian skull vault. *Dev Biol* 241:106–16.
- Johnston MC, Bhakdinaronk A, Reid YC. 1973. An expanded role of the neural crest in oral and pharyngeal development. In: Bosma JF, editor. Fourth symposium on oral sensation and perception: development in the fetus and infant. Bethesda: US Department of Health, Education, and Welfare. p. 37–52.
- Jollie MT. 1977. Segmentation of the vertebrate head. *Amer Zool* 17:323–33.
- Jurgens JD. 1971. The morphology of the nasal region of Amphibia and its bearing on the phylogeny of the group. *Ann Univ Stellenbosch, Ser A*, 46:1–146.
- Köntges G, Lumsden A. 1996. Rhombencephalic neural crest segmentation is preserved throughout craniofacial ontogeny. *Development* 122:3229–42.
- Kuratani S. 2003. Evolutionary developmental biology and vertebrate head segmentation: a perspective from developmental constraint. *Theory Biosci* 122:230–51.
- Kuratani S. 2005. Craniofacial development and the evolution of the vertebrates: the old problems on a new background. *Zool Sci* 22:1–19.
- Kuratani S, Ota KG. 2008. Primitive versus derived traits in the developmental program of the vertebrate head: views from cyclostome developmental studies. *J Exp Zool (Mol Dev Evol)* 308B:294–314.
- Landacre FL. 1921. The fate of the neural crest in the head of urodeles. *J Comp Neurol* 33:1–43.
- Le Douarin N, Barq G. 1969. Use of Japanese quail cells as “biological markers” in experimental embryology. *C R Acad Sci Hebd Seances Acad Sci D* 269:1543–6.
- Le Douarin NM, Kalcheim C. 1999. The neural crest. Cambridge: Cambridge University Press. p. 445.
- Le Lièvre CS. 1974. Rôle des cellules mésectodermiques issues des crêtes neurales céphaliques dans la formation des arcs branchiaux et du squelette viscéral. *J Embryol Exp Morph* 31:453–77.
- Le Lièvre CS. 1978. Participation of neural crest-derived cells in the genesis of the skull in birds. *J Embryol exp Morph* 47:17–37.
- Luther A. 1925. Entwicklungsmechanische Untersuchungen am Labyrinth einiger Anuren. *Soc Scient Fenn Comm Biol* 11:1–48.
- Mason MJ, Narins PM. 2002. Vibrometric studies of the middle ear of the bullfrog *Rana catesbeiana* I. The extrastapes. *J Exp Biol* 205:3153–65.
- Matsuoka T, Ahlberg PE, Kessarri N, Iannarelli P, Dennehy U, Richardson WD, McMahon AP, Koentges G. 2005. Neural crest origins of the neck and shoulder. *Nature* 436:347–55.
- Morriss-Kay GM. 2001. Derivation of the mammalian skull vault. *J Anat* 199:143–51.
- Moury JD, Hanken J. 1995. Early cranial neural crest migration in the direct-developing frog, *Eleutherodactylus coqui*. *Acta Anat* 153:243–53.
- Nakajima K, Fujimoto K, Yaoita Y. 2005. Programmed cell death during amphibian metamorphosis. *Sem Cell Dev Biol* 16:271–80.
- Nieuwkoop PD, Faber J. 1994. Normal table of *Xenopus laevis* (Daudin). New York and London: Garland Publishing Inc. p. 252.
- Noden DM. 1978. The control of avian cephalic neural crest cytodifferentiation I. Skeletal and connective tissues. *Dev Biol* 67:296–312.
- Noden DM. 1982. Patterns and organization of craniofacial skeletogenic and myogenic mesenchyme: a perspective. In: Dixon AD, Sarnat BG, editors. Progress in clinical and biological research: factors and mechanisms influencing bone growth. New York: A. R. Liss. p. 167–203.
- Noden DM. 1983. The role of the neural crest in patterning avian cranial skeletal, connective, and muscle tissues. *Dev Biol* 96:144–65.
- Noden DM. 1984. The use of chimeras in analyses of craniofacial development. In: Le Douarin NM, McLaren A, editors. Chimeras in developmental biology. London: Academic Press. p. 241–80.
- Noden DM. 1987. Interactions between cephalic neural crest and mesodermal populations. In: Maderson PFA, editor. Developmental and evolutionary aspects of the neural crest. New York: John Wiley & Sons. p. 89–119.
- Noden DM. 1988. Interactions and fates of avian craniofacial mesenchyme. *Development* 103(Suppl.):121–40.
- Olsson L, Hanken J. 1996. Cranial neural-crest migration and chondrogenic fate in the Oriental fire-bellied toad *Bombina orientalis*: defining the ancestral pattern of head development in anuran amphibians. *J Morphol* 229:105–20.
- Olsson L, Moury JD, Carl TF, Håstad O, Hanken J. 2002. Cranial neural crest-cell migration in the direct-developing frog, *Eleutherodactylus coqui*: molecular heterogeneity within and among migratory streams. *Zoology* 105:3–13.
- O’Rahilly R, Muller F. 1984. The early development of the hypoglossal nerve and occipital somites in staged human embryos. *Am J Anat* 169:237–57.
- Owen R. 1866. On the anatomy of vertebrates. Fishes and reptiles, Vol. I. London: Longmans, Green. p. 915.
- Piekarski N, Olsson L. 2007. Muscular derivatives of the cranialmost somites revealed by long-term fate mapping in the Mexican axolotl (*Ambystoma mexicanum*). *Evol Dev* 9:566–78.
- Platt JB. 1893. Ectodermic origin of the cartilages of the head. *Anat Anz* 8:506–9.
- Presnell J, Schreibman M. 1997. Humason’s animal tissue techniques. Baltimore: The Johns Hopkins University Press. p. 572.

- Pugener LA, Maglia AM. 2007. Skeletal morphology and development of the olfactory region of *Spea* (Anura: Scaphiropodidae). *J Anat* 211:754–68.
- Reiss OJ. 1998. Anuran postnasal wall homology: an experimental study. *J Morphol* 238:343–53.
- Sadaghiani B, Thiébaud CH. 1987. Neural crest development in the *Xenopus laevis* embryo, studied by interspecific transplantation and scanning electron microscopy. *Dev Biol* 124:91–110.
- Sedra SN, Michael MI. 1957. The development of the skull, visceral arches, larynx, and visceral muscles of the South African clawed toad, *Xenopus laevis* (Daudin) during the process of metamorphosis. *Verh K Akad Wet Amsterdam Afd Naturkd* 51:1–80.
- Sedra SN, Michael MI. 1959. The ontogenesis of the sound conducting apparatus of the Egyptian toad, *Bufo regularis* Reuss, with a review of this apparatus in Salientia. *J Morphol* 104:359–75.
- Sive HL, Grainger RM, Harland RM. 2000. Early development of *Xenopus laevis*. Cold Spring Harbor: Cold Spring Harbor Laboratory Press. p. 338.
- Smit AL. 1953. The ontogenesis of the vertebral column of *Xenopus laevis* (Daudin) with special reference to the segmentation of the metotic region of the skull. *Ann Univ Stellenbosch, Ser A*, 29:81–136.
- Stone L. 1926. Further experiments on the extirpation and transplantation of mesectoderm in *Ambystoma punctatum*. *J Exp Zool* 44:95–131.
- Stone L. 1929. Experiments showing the role of migrating neural crest (mesectoderm) in the formation of head skeleton and loose connective tissue in *Rana palustris*. *Wilhelm Roux Arch Dev Biol* 118:40–77.
- Swanepoel JH. 1970. The ontogenesis of the chondrocranium and of the nasal sac of the microhylid frog *Breviceps adspersus pentheri* Werner. *Ann Univ Stellenbosch, Ser A*, 45:1–119.
- Tata JR. 1994. Hormonal regulation of programmed cell death during amphibian metamorphosis. *Biochem Cell Biol* 72:581–8.
- Toerien MJ. 1963. Experimental studies on the origin of the cartilage of the auditory capsule and columella in *Ambystoma*. *J Embryol Exp Morphol* 11:459–73.
- Trueb L, Hanken J. 1992. Skeletal development in *Xenopus laevis* (Anura: Pipidae). *J Morphol* 214:1–41.
- van der Westhuizen CM. 1961. The development of the chondrocranium of *Heleophryne purcelli* Sclater with special reference to the palatoquadrate and the sound-conducting apparatus. *Acta Zool Stockholm* 42:1–72.
- Violette HN. 1930. Origin of columella auris of Anura. *Anat Rec* 45:280.
- Wagner G. 1949. Die Bedeutung der Neuralleiste für die Kopfgestaltung der Amphibienlarven: Untersuchungen an Chimären von *Triton* und *Bombinator*. *Rev Suisse Zool* 56:519–620.